From transcriptomics to metabolomics: Extracellular ATP induces TGF-β-like and TGF-β-independent epithelial mesenchymal transition in lung cancer cells

Maria Evers
Ohio University
Jingwen Song
Ohio University
Pratik Shriwas
Ohio University
Harrison S Greenbaum
University of Chicago Biological Sciences Division: University of Chicago Division of the Biological Sciences
Xiaozhuo Chen (chenx@ohio.edu)
Ohio University https://orcid.org/0000-0001-9635-4572

Research

Keywords: Epithelial mesenchymal transition (EMT), transcriptomics, metabolomics, Extracellular ATP

Posted Date: April 9th, 2021

DOI: https://doi.org/10.21203/rs.3.rs-403352/v1

Abstract

Background: Epithelial mesenchymal transition (EMT) is an early process in metastasis. Extracellular ATP (eATP) was shown to play important roles in EMT. However, the mechanisms by which eATP induces EMT and ATP's relationship to TGF-b, a well-known EMT inducer, are unclear. Key questions include: if and how much EMT-specific gene expression eATP induces and how similar is ATP-induced EMT to TGF-b-induced EMT? We hypothesized that eATP acts as a specific inducer and regulator of EMT at all levels alternative to TGF-b in cancer cells.

Methods: As EMT involves changes from gene expression to metabolites, RNAseq and metabolomics analyses were performed on human NSCLC A549 cells treated with either eATP or TGF-b to determine how they induce EMT at transcription and metabolic levels. Bio-functional assays, such as Transwell invasion, intracellular ATP, resazurin cell viability, fluorescence microscopy of filopodia formation, and antibody neutralization / cell rescue, were conducted in more NSCLC cell lines to validate changes identified from RNAseq and metabolomics analyses by confirming the corresponding EMT phenotypic changes.

Results: RNAseq analysis shows that eATP significantly enriched expressions of genes involved in EMT temporarily, and similarly but non-identically to TGF-b after 2 and 6 hours of treatment. Eleven genes, with known or unknown functions in EMT, are significantly upregulated by both inducers at both time points, have been identified. Metabolomics analysis revealed eATP induced numerous EMT-related changes in metabolic pathways, including cytoskeleton rearrangement, glycolysis, glutaminolysis, ROS, and individual metabolic changes similar or identical to those induced by TGF-b. eATP-induced transcriptomic changes appeared smaller but earlier than TGF-b. Functional bioassays verified the RNAseq and metabolomics findings that eATP induced earlier and more invasion and formation of filopodia in A549 and H1299 cells, and restored viability of cancer cells treated with TGF-b-neutralizing antibodies.

Conclusions: eATP-induced EMT, from gene expression changes and metabolic reprogramming, is similar but non-identical to that induced by TGF-b, and is independent of TGF-b. The smaller but earlier EMT-related changes induced by eATP, compared with TGF-b, could be largely explained by extracellular action of eATP and intracellular activities of macropinocytosis-internalized eATP. These strongly indicate that eATP is an emerging master inducer and regulator of EMT.

Background

Metastasis is associated with up to 90% of all cancer-related death [1] but is also one of the least understood processes in cancer. Metastasis starts with a process known as epithelial to mesenchymal transition (EMT), in which a group of epithelial (E) related genes in cancer cells are downregulated and phenotypes suppressed while some mesenchymal (M) genes are upregulated and M phenotypes are expressed [2, 3], in preparation for subsequent invasion and metastasis. EMT also occurs in normal processes such as early embryonic development when cell migration and cell differentiation are required

[3]. EMT in cancer cells appear to be a “hijacked” process that mimics EMT in normal cells to achieve their own purpose of increased survival.

EMT itself is a complicated and partially understood process that involves various sub-steps with each corresponding change in cell signaling, gene expression, metabolism, morphology, motility, and cell functions [4, 5]. In addition, cells of different cancer types have been shown to respond to various kinds of stimuli and express somewhat different sets of genes to reach a general state termed partial EMT [6–8]. In a partial EMT state, which happens in all cancer cells examined upon EMT induction, cancer cells of different cancer types upregulate an incomplete and somewhat different set of mesenchymal genes and downregulate an incomplete and different set of epithelial genes depending upon cancer types, induction conditions, and tumor microenvironmental cues [6–8]. Exactly how EMT is induced and regulated in cancer is far from fully understood, but TGF-b has long been recognized as a major EMT inducer and regulator [9–10]. TGF-b binds and activates cell membrane-associated TGF-b receptors. The activation of TGF-b receptors results in cascades of intracellular signaling, leading to EMT-related gene expression, metabolic reprograming, and phenotypic changes [11, 12]. One of the TGF-b signaling pathways and induced processes described in cancer cells is the exocytosis of cytosolic ATP-containing vesicles, releasing ATP to the extracellular environment and creating an autocrine / paracrine signaling loop through extracellular binding and activating of purinergic receptors (PR) located on plasma membrane of cancer cells [13, 14]. PR signaling by ATP is vitally important for inducing EMT [15]. However, ATP-PR signaling is only one of the several signaling pathways induced by TGF-b, and it remains unclear if extracellular ATP alone is sufficient to induce EMT at levels from transcription to metabolism.

Ample evidence strongly suggests that extracellular ATP (eATP) plays very important roles in EMT and metastasis. First, intratumoral eATP (ieATP) in the tumor microenvironment (TME) has been found to be in a concentration range of 10^3 to 10^4 times higher than those in normal tissues (16–19), between ~ 200–600 mM. Previously, we reported that eATP, at the reported intratumoral concentrations, was internalized by macropinocytosis, a special form of endocytosis [20–22], both in vitro and in vivo in cancer cells of various cancer types [23–26]. The internalized ATP greatly elevates intracellular ATP levels, which in turn increases the cancer cell proliferation rate and resistance to anticancer drugs, including those target drugs that compete with ATP for the ATP binding site of the protein targets [27, 28]. More recently, we have reported the observation of eATP-induced EMT, including cell detachment, cell migration and invasion, morphologic and motility changes, and protein expression alterations in human NSCLC A549 cells [29]. In addition, ATP is a transcription cofactor involved in various steps of the transcription process, such as initiation, elongation, termination and more, to speed up gene expression [30–34]. However, if / how much eATP induces corresponding changes at either the gene expression or metabolic level during the EMT process have never been fully investigated, let alone investigated together. In addition, the similarities and differences between eATP and TGF-b in EMT induction at these levels were never compared.

In this study, we hypothesized that eATP functions as key master inducer and regulator of EMT either in parallel or alternative to TGF-b, at all biological levels in cancer cells. Thus, we combined RNA sequencing

[35, 36] with metabolomics analyses to test this hypothesis in A549 cells at the levels of gene expression and metabolites and verified these results with functional studies. These studies were included because EMT is characterized by the expression of specific genes with subsequent metabolic reprogramming in cancer cells. These metabolites are the end products of EMT induction and correspond to the phenotypic changes associated with EMT. We then performed various bio-functional assays, such as invasion, cell morphological changes, and cell viability, to characterize cellular and functional changes for supporting, confirming and validating eATP-induced and -regulated EMT demonstrated by RNAseq and metabolomics analyses. We used TGF-b as a known EMT inducer and TGF-b treated NSCLC cell lines as cell controls for comparison. The potentially mutual regulatory activities between eATP and TGF-β were also investigated, as they shared some apparently redundant activities in EMT induction. In addition, we evaluated the importance and contribution of eATP-enhanced intracellular ATP concentrations in eATP-induced EMT. The results of these studies show significant and independent contribution to and profound implications of eATP in EMT and potentially in metastasis.

Materials And Methods

Chemicals, Proteins, and Antibodies

Cell culture reagents were purchased from VWR. ATP was purchased from Sigma-Aldrich. TGF- β1 protein was from Cell Signaling. Pan-neutralizing antibody against TGF-β ligands was from Cell Signaling.

Cell Lines and Cell Culture

Human non-small cell lung cancer (NSCLC) cell lines A549 and H1299 were purchased from ATCC. A549 and H1299 cells were cultured in Dulbecco's Modified Eagle Medium (DMEM) as previously described [25–29].

We chose human lung cancer A549 and H1299 cells for the study because lung cancer has been our lab's major cancer target and these two NSCLC cell lines have been used in our and other labs frequently before [24–27].

RNA Sequencing

Sample preparation: A549 cells were treated by ATP or TGF-b for 2 or 6 hrs because we were primarily interested in catching early to mid-stage gene expression which are responsible for the induction of EMT. In addition, preliminary data showed a pattern of several EMT-TF levels peaking 6 hours post treatment (unpublished observation). After treatment, RNA was isolated from cells using an RNA Isolation kit (Thermo Fisher) following manufacturer's instructions. Genomic DNA was removed from the samples using a genomic DNA removal kit (Thermo Fisher). RNA samples were eluted in DEPC treated water (Thermo Fisher). RNA Integrity number values were measured by the Ohio University Genomics Facility to ensure quality of the RNA before samples were shipped to LC Sciences in Houston, TX, for a total polyA RNA sequencing.

RNA sequencing data analysis. A complete transcriptome was assembled after the sequencing and the primary analysis of the transcriptome provided by the company were further analyzed to identify gene expression changes associated with EMT induction. Analyses were performed to identify gene sets that were enriched in ATP and TGF-β treated cells, and gene sets were considered significantly enriched if their false discovery rate (FDR) q value was < 0.10, which is 15% less than the value recommended by the GSEA user guide (< 0.25). Heat map genes were identified from GSEA enrichments [37–39]. Identified genes expression levels were averaged between samples, gene names were converted from ensemble transcript ID to universal gene symbol using the DAVID database [40, 41], and top hits were visualized utilizing Morpheus heatmapping software form the Broad Institute [https://software.broadinstitute.org/morpheus].

Metabolomics analysis

Sample preparation: Treatment times of 2, 6, and 12 hours were chosen for the reasons of matching with the RNAseq conditions (2 and 6 hr) and including a condition of late stage EMT (12hr). A549 cells were treated as follows: no treatment/control, .5 mM eATP, and 10 ng/mL TGF-β. Cell culture metabolism was stopped by briefly incubating in ddH_2O, metabolites were extracted by 80% ice cold methanol, and samples were sonicated and centrifuged at 4°C. Metabolites are present in the supernatant, which was removed and freeze dried [42]. Samples were stored in -80°C and analyzed at the Ohio State University Campus chemical instrumentation center (CCIC).

Metabolomics data analysis: Metabolomics study was completed by quantitative untargeted LC-MS utilizing Q-TOF 6545 mass spectrometer connected to an Agilent 1290 UHPLC system with a Poroshell 120 SB-C18 (2 × 100 mm, 2.7-μm particle size) column. Metabolomics data was generated and received from CCIC. Masshunter software (Agilent Technology) was used for acquiring data and peaks were integrated using Progenesis (Agilent Technology). Compounds were identified with XCMS as well as Metaboanalyst 5.0 software. Peak areas were normalized using internal standards and were subjected to relative quantification analyses with control (no treatment).

Invasion assays

Cancer cell invasion assays were performed as previously described with a more extensive dose-dependent studies [29]. The cells were incubated under different conditions (to both the upper and lower chambers) including: 1) control/no treatment, .1 mM ATP, .2 mM ATP, .3 mM ATP, .4 mM ATP, .5 mM ATP, 2) control/no treatment, .25 mM ATP, .5 mM ATP, .75 mM ATP, 5 ng/ml TGF-b, 10 ng/ml TGF- b, 3) no treatment/control, .5 mM ATP, 10 ng/ml TGF- b, .5 mM ATP + 10 ng/ml TGF- b, 4) no treatment/control, .1 mM ATP, 3 ng/ml TGF- b, .1 mM ATP + 3 ng/ml TGF- b, 5) no treatment/control, .25 μg/ml TGF-β antibody, .50 μg/ml TGF-β antibody, .75 μg/ml TGF-β antibody, .25 μg/ml TGF-β antibody + .5 mM ATP, .50 μg/ml TGF-β antibody + .5 mM ATP, .75 μg/ml TGF-β antibody + .5 mM ATP. After 20 hours incubation at 37°C, invaded cells to the bottom (opposite side) of the polycarbonate membrane of the upper insert were fixed with 4% paraformaldehyde and stained with crystal violet, and visually counted from six representative visual fields per well in experimental triplicate using compound light microscopy (200X magnification),

and then averaged. The TGF-b concentrations used in these assays were the commonly reported ones in the literature.

Fluorescence microscopy of eATP treated cancer cells

To observe morphological changes of filopodia-like protrusions, fluorescence microscopy was performed as previously described with an extensive time-dependent study [29]. Briefly, F-actin (filamentous-actin) of cells were stained with Fluorescent Phallotoxins. A549 or H1299 cells were seeded overnight on glass coverslips placed in 24-well plates, then treated with or without ATP or TGF-b for various time periods (2, 6, and 12 hours). Stained cells were examined and photographed using a Fluor Motorized DIC Polarization Phase Contrast Microscope (Zeiss AXIO Observer) at 200× magnification.

ATP assay

The intracellular ATP levels were measured as described previously [24–26]. A549 or H1299 cells were treated with 5 and 10 ng/ml TGF-β for 6 hours, or various concentrations of ATP (ranging from 10 to 500 μM) for 24 hours. iATP levels were measured using an ATPlite luminescence assay system (Perkin Elmer) according to manufacturer's instructions. In addition to the treatment groups, a 0-hour negative control was included for indicating the baseline. A 6-hour incubation time was chosen for the TGF-β treatment for this study because preliminary data generated in our lab has identified that mRNA levels for transcription factors associated with EMT and cancer stem cells peak around 6 hours after ATP treatment (unpublished data). A 24-hour incubation time was chosen because previous studies have shown this is an adequate amount of time for macropinocytosis to occur and reach equilibrium [25, 26].

Cell viability assay

Cell viability was measured using a Resazurin Assay. A549 cells were treated as follows: no treatment/control, .25 μg/ml TGF-β antibody, .50 μg/ml TGF-β antibody, .75 μg/ml TGF-β antibody, .25 μg/ml TGF-β antibody + .5 mM ATP, .50 μg/ml TGF-β antibody + .5 mM ATP, .75 μg/ml TGF-β antibody + .5 mM ATP, and .5 mM ATP for 24 hours. Media was aspirated from cells and replaced with fresh media containing 0.0045% of resazurin dye. Cells were incubated at 37°C for 10 minutes and the plate was read with a fluorescence microplate reader (Citation 3, BioTek) with excitation at 570 nm and emission at 590 nm.

Western Blot Analysis

Proteins were isolated from cells treated with no treatment, .5 mM ATP for 2 hours or 6 hours, or 10 ng/ml TGF-b for 2 hours or 6 hours. Proteins were analyzed with western blots using appropriate primary rabbit anti-human antibodies all purchased from Cell signaling Technologies: E-cadherin (# 3195), Snail (#3879), Vimentin (# 5741), MMP-1 (#54376), MMP-3 (# 14351), MMP-9 (# 2270), Claudin-2 (# 48120), and NF-kBp65 (# 4764). Secondary antibody staining was completed with anti-rabbit IgG, HRP-linked antibody (Goat, 1:1000, CST, #7074). Cofilin (D3F9) XP® Rabbit mAb (#5175) was used as a protein loading control. The signals were detected with Super Signal West Pico Chemiluminescent substrate

(Thermo Fisher Scientific) and was developed using (Odyssey Fc 2800, LI-COR Biosciences). Intensities of protein bands were quantified by the corresponding Odyssey Fc software used to develop blots.

Data Analysis

Each experimental condition will be performed in at least triplicates and repeated at least once. Results were reported as mean ± standard deviation. The statistical difference, or difference between control and treatment groups, was analyzed using Student's t-test or one-way ANOVA. $P < 0.05$ was considered statistically significant.

Results

RNA Sequencing reveals that eATP induces gene expression similar but not identical to those induced by TGF-b

First, we wanted to determine if and how eATP induces changes at the gene expression level as compared with TGF-b. Such a study was never done at the transcriptome level. To that end, RNA sequencing (RNAseq) analysis was performed (Fig. 1a).

At 2 hours of treatment, TGF-β significantly upregulated a total of 613 genes while eATP upregulated 394 genes (Fig. 1b left). In addition, among these genes, 131 genes induced by both molecules were identical. At 6 hours, TGF-β induced 648 genes whereas eATP induced 135 genes. Between 2 hours and 6 hours, TGF-β significantly induced roughly the same number of genes while eATP significantly induced only about 1/3 of the genes at 6 hours compared with those of 2 hours. At 6 hours, 42 genes significantly upregulated by both inducers remained identical. These large changes over time in the eATP-induced gene expressions correlate with the invasion and morphology changes induced by eATP (Figs. 3 & 4).

In comparison, at 2 hours, TGF-β significantly downregulated 229 genes while eATP downregulated 177 genes (Fig. 1b right). At 6 hours, TGF-β significantly downregulated 612 genes. In contrast, eATP significantly downregulated 146 genes, a small decrease compared with its 2-hour counterpart (Fig. 1b right).

In the gene set enrichment analysis (GSEA) plots for the "Hallmark - Epithelial mesenchymal transition" signature, EMT is more enriched at 2 hours (Fig. 1c) and at 6 hours (Fig. 1d) for both eATP and TGF-b treatments compared to the untreated controls. Comparisons between 2 and 6 hours of the same treatment show that EMT is more enriched at 2 hours than 6 hours for ATP (Fig. 1e), while EMT is more enriched for TGF-b at 6 hours than two hours (Fig. 1f), suggesting that EMT enrichment / progress induced by ATP is earlier/faster than that for TGF-b. From the gene set enrichment analysis, we found the top 20 most enriched genes in common between ATP and TGF-b at both 2 hours and 6 hours (Fig. 1g and 1h). The results from the top 20 enriched genes are consistent with ATP appearing to induce EMT earlier than TGF-b. EMT related genes were more enriched by ATP induction at 2 hours (Fig. 1g) while TGF-b induced genes were more enriched than ATP at 6 hours (Fig. 1h). Thus, the heatmap results are consistent with the enrichment analyses (Fig. 1e & 1f), again confirming that ATP appears to induce EMT

enrichment earlier than TGF-b. In addition, enrichment analysis showed that TGF-β had significantly more genes enriched for EMT in comparison to ATP at 6 hours (Fig. S1a, right), but not at 2 hours (Fig. S1b, left).

Eleven genes were upregulated and conserved in inductions by both eATP and TGF-b

Both eATP and TGF-b induced significant upregulation of a common set of 11 genes at both 2 and 6 hours of treatment (Table 1, top half). Among these 11 genes, several are well-known to be involved in EMT, such as Sox8, BMP6, MMP10, and others. Several other genes, however, are less well known or not currently known to be associated with EMT. These include *STC1*, *GJB3*, and *BLOC1S6*. Intriguingly, ATP6V1G2-DDX39B, a long non-translated fusion RNA, was also conserved in this group. This readthrough transcript contains an ATPase gene and the *DDX39B*, an RNA splicing gene, raising questions as how this RNA participates in the induction and regulation of EMT.

RNAseq analysis also identified 7 genes that were conserved and significantly downregulated by both eATP and TGF-b at both times (Table 1, bottom half). Some of these genes or long non-protein coding transcripts are also unknown for their functions in EMT.

Metabolomics analyses of eATP treated A549 cells show changes associated with EMT

Metabolic profiles of eATP- or TGF-b-treated cancer cells induced at various times are “snapshots” of cancer cells’ total sum of metabolic changes and reflections of metabolic and phenotypic changes during EMT induction at those time points. For these reasons, the metabolomics study was conducted (Fig. 2a). Partial least-square discriminant analysis (PLS-DA) was performed on the data collected by performing negative ion mode LC-MS/MS. The PLS-DA analysis showed that control treated A549 cancer cells could be separated (based on their metabolite abundances) from ATP- and TGF-b-treated cells after 2, 6 and 12 hours of treatment (Fig. 2b). Similarly, PLS-DA analysis was performed on data collected by positive ion mode (Fig. S2).

Metabolic pathway enrichment analyses show that, among the 25 most enriched pathways in each treatment, about half of those pathways are either identical or similar between control vs 2hr ATP and control vs 2hr TGF- β treated A549 cells (Fig. 2c and 2d). Those identical metabolic pathways are concentrated in the glucose metabolism area, including glycolysis / gluconeogenesis, TCA cycle, glutamine, pyruvate, and purine. TGF-b induces these for EMT [11, 12]. These pathways are known to be inducers of EMT and thus this shows similarity in alterations induced by ATP and TGF- β in A549 cell metabolism.

eATP induced similar cell invasion to TGF-b in two human lung cancer cell lines tested

Transwell assays showed that the invasion rates were eATP dose-dependent in both A549 cells (Fig. S3a) and H1299 cells (Fig. S3b). Transwell invasion assays show that eATP induced dose-dependent invasions similar to TGF-β in NSCLC cell lines A549 (Fig. 3a) and H1299 cells (Fig. 3b). Gene set enrichment analysis (GSEA) reveals that genes involved in cell migration (Fig. 3c) and in negative cell adhesion regulation (Fig. 3d) were significantly enriched by eATP and TGF-b, supporting the increased invasion, compared with the untreated controls, induced by both molecules.

Western blot analysis indicated that selected E-type proteins were in general downregulated while M-type proteins were upregulated by eATP, and eATP induced changes are in general in the same direction as TGF-b (Fig. 3e) and its quantification of Fig. S3c), further supporting the role of eATP in EMT induction.

Finally, the increased invasion was confirmed by the metabolomics analysis of invasion/migration-related metabolites, whose abundances were altered in a similar way in both 2hr ATP- and 2hr TGF-b induced samples (Fig. 3f). These results also indicate that invasion as an EMT-required phenotypes could be induced by eATP in the range of eATP concentrations found in TME [16–19].

eATP induced formation of filopodia-like protrusions earlier than TGF-b in two human lung cancer cell lines

Filopodia are “feet-like” cell structures necessary for cell migration and invasion and are a cellular morphology feature induced in EMT. We previously demonstrated eATP-induced formation of filopodia-like protrusions in A549 cells [29]. But we did not know when the protrusions were induced or if the timing of protrusion formation induced by eATP or TGF-b differ from each other. The time course study revealed that the protrusions were formed as early as 2 hours in A549 cells treated with eATP and h persist for at least 12 hours (Fig. 4a). In comparison, the formation in the TGF-b treated A549 cells was noticeably slower. Similar changes were also observed in H1299 cells (Fig. 4b) with the difference of some protrusions being formed even without eATP or TGF-b treatment. The pre-existing protrusions in H1299 cells were previously documented [43]. TGF-β concentrations used in these assays were most commonly reported in the literature. This assay provides a visual evidence for the first time that eATP induces time-dependent cellular morphology changes needed for EMT and invasion, further confirming and supporting the notion that eATP induced earlier invasion capability than TGF-β.

RNAseq GSEA analysis shows that actin-cytoskeleton reorganization related genes are enriched 2 hours after ATP or TGF-b treatment (Fig. 4c). The top 20 enriched genes in common between ATP and TGF-β for actin cytoskeleton reorganization show similar changes (Fig. 4d). Metabolomics analysis on cell actin-cytoskeleton rearrangement showed that, among 12 metabolites in this group, 11 metabolites show concentration changes induced by eATP, either increased or decreased, in the same direction compared with TGF-b induction relative to the control at 2 hours (Fig. 4e). These metabolites are known to be changed in EMT. Thus, these results indicate that actin-cytoskeleton rearrangement has occurred in these cells treated with either molecule as a result of EMT.

ATP and TGF-β show additive effects on cell invasion at lower concentrations but not at higher concentrations

At concentrations significantly lower than their respective optimal concentrations for EMT induction, the combined treatment of eATP and TGF- b produced more invasion than the individual treatment alone (Fig. 5a). However, this additive effect disappeared when regular concentrations were used (Fig. 5b), suggesting that eATP and TGF-b are very likely to act by using, at least in part, the same pathways for inducing invasion. Both eATP and TGF-b are known to use purinergic receptor signaling for their EMT induction [13–15].

eATP restored invasiveness of A549 cells reduced by antibodies against TGF-β

To further test the hypothesis that eATP induces EMT using mechanism(s) similar to those of TGF-β, a cell viability assay was conducted. This assay result revealed that normal cell proliferation and cell viability were not stopped in A549 cells (Fig. 5c) by the addition of TGF-β antibody, but the cell viability was further increased by the addition of eATP (Fig. 5c). In comparison, cell invasiveness was reduced by TGF-b neutralizing antibody treatment but the reduced invasiveness was restored by the addition of ATP (Fig. 5d). These results strongly suggest that eATP restored the activities, blocked by the antibody, by increasing cell invasiveness using mechanisms either similar to or different from those used by TGF-β. ATP induced mechanism(s) is capable of bypassing the action of the TGF-b receptor. These results are consistent with those found in invasion studies (Fig. 3), cell morphology studies (Fig. 4), and the additive effect study (Fig. 5a and 5b).

RNAseq analysis revealed that, after 2 hours of treatment, a set of genes involved in EMT were enriched by TGF-β but not by ATP (Fig. 5), while another set of EMT genes were enriched by eATP but not by TGF-b (Fig. 5g). These results, in combination with Fig. 1g and 1h, show that ATP and TGF-b use partially similar and partially different genes to induce EMT, providing an explanation for the additive effect observed at low doses and ATP's ability to rescue invasion when TGF-β signaling is not present.

Extracellular ATP induces dose-dependent elevation of intracellular ATP concentrations while TGF-β does not.

To compare the similarities and differences between eATP and TGF-b in their respective mechanisms in EMT induction, the treatment followed by intracellular ATP (iATP) measurements were performed. The assay showed that eATP induced dose-dependent elevation of iATP concentrations in A549 cells (Fig. 6a) while TGF-b treatment did not change iATP level (Fig. 6b). The same result was observed in H1299 cells (Fig. S4a and S4b). These results suggest that, although eATP induces EMT by possibly using similar mechanisms used by TGF-b, eATP actions are aided by increased iATP concentration. In contrast, TGF-b's EMT-inducing mechanisms do not involve iATP level elevation. Therefore, the differences in iATP levels may account for the differences observed in the invasion and filopodia formation induced by the two molecules (Figs. 3 and 4), since iATP can function as either an energy source for cell movement, a phosphate donor, a signal amplifier in signal transduction, and even a transcription cofactor.

eATP induced transcriptomics and metabolomics changes in ROS pathways and corresponding metabolites

Glycolysis, glutaminolysis, and TCA cycle are known to be altered during EMT [11]. Most of the metabolites in glycolysis and glutaminolysis changed their concentrations in the same direction 2 hours after the treatment by either ATP or TGF-b (Fig. 6c). Larger differences can be found in the TCA cycle metabolism (Fig. 6d). This may be due to the fact that one key function of the TCA cycle is for mitochondrial ATP synthesis but this synthesis is largely unnecessary for the eATP-treated cells because of the macropinocytosis mediated eATP internalization. Thus, it is not surprising that control and eATP treated samples were clustered eATP together much more than TGF-b-treated samples.

ROS is well known to be involved in EMT [11]. Metabolomics analysis reveals that concentrations of major metabolites in the ROS pathway changed to the same direction in both ATP- and TGF-b-treated samples after 2 hours of treatment (Fig. 7a), indicating an increasing ROS status.

GSEA of RNAseq data also show that response to oxidative stress, cellular response to ROS, and superoxide metabolic processes are enriched (Fig. 7b, 7c, and 7d), matching and supporting the metabolic finding.

This indicates that, regarding the ROS and oxidative stress status, eATP-induced and TGF-b-induced cells were in very similar metabolic state, presumably an EMT state.

Based on all these new findings and our previous findings, we propose a new hypothetical model to explain the mechanisms used by eATP to induce EMT (Fig. 7e).

Discussions

Several unique features of eATP and macropinocytosed eATP support them as being a potential master inducer and regulator of EMT. First, ATP is an extracellular messenger for activating purinergic receptor (PR) mediated signaling, which has been implicated in EMT [44–46], providing the basis for specificity for ATP-triggered signaling and actions. ATP is a protein phosphorylation donor participating in almost all intracellular signaling pathways. In PR signaling, eATP not only induces PR activation, but also enhances PR signaling by providing extra phosphate donors when eATP is internalized to elevate intracellular ATP concentrations. Second, ATP is also a versatile transcription cofactor, participating in a wide variety of transcriptional activities such as DNA unwinding, transcription initiation, elongation, and termination [30–34]. Furthermore, ATP is also a cofactor in energy-required enzymatic reactions, accelerating reaction rates. These properties make ATP stand out as a potential inducer and regulator for EMT, a process that relies on well-regulated changes in signal transduction, gene expression (transcription), translation, and metabolism. More directly related to cell motility and metastasis, ATP is a well-known danger signal for bacteria and cancer cells [47, 48]. Elevated ATP concentrations in the environment functions as a warning signal to bacteria and animal cells for the incoming danger and telling them to flee for a safer environment. Apparently, this conserved activity is hijacked and utilized by cancer cells to signal

imminent danger of their original sites within tumors when the conditions in TME is deteriorating due to hypoxia and shortage of nutritional supply. It is conceivable that eATP-induced EMT is one of the mechanisms utilized by cancer cells in tumors preparing cancer cell and enabling them for departure, reseeding in the same tumor, invasion and even metastasis. Some major remaining questions include: how much, at what levels, at what cellular locations, and in what relationship to TGF-b, eATP participates in EMT? Our current study was one of the first steps towards answering these key questions for better understanding of the EMT induction process by using a combinatorial study strategy of RNAseq, metabolomics, and functional assays.

The Venn graphs of the RNAseq analysis show that, like TGF-b, eATP upregulated many genes, and downregulated many other genes. Most of these genes are upregulated or downregulated similarly by eATP and TGF-b (Table 1), strongly suggesting that eATP induced and regulated the same process as TGF-b, namely EMT. These changes also indicate that the eATP treatment did not randomly induce gene expressions but only those related to and needed for EMT. Secondly, also like TGF-b, eATP exhibited time-dependent gene expressions. The 6-hour treatment led to an appearance of the expression of some new genes that did not show up at the 2-hour treatment and a disappearance of the expression and downregulation of some other genes. These expression pattern changes suggest that eATP not only induces EMT, but also temporally regulates EMT, orchestrating the progress by expressing the right genes at the right times and at right levels.

On the first look, eATP induced fewer significant changes in upregulated and downregulated genes compared with TGF-β. A closer examination of the RNAseq data reveals that eATP induced changes of expression in about as many genes as TGF-β, but just not to the level of statistical significance determined by the RNAseq software (unpublished observations). Similar phenomenon was also observed in metabolomics data (Fig. 4e and 5d). The multi-functionality and multi-locality of ATP and internalized eATP might be behind the apparent differences. It is possible that the elevated iATP concentrations (Fig. 5d) drive the accelerated signal transduction and biochemical reactions while maintaining the expression of the enzyme genes and metabolites involved in these reactions at levels lower than those found in TGF-β-treated cells (Table 1, and Fig. 4e and 5d).

For some of those M-type genes significantly altered by both eATP and TGF-b, eATP-induced genes tend to show higher Log2fc values at 2 hr than those induced by TGF-b, while genes induced by TGF-b tend to have higher Log2fc values at 6 hr than eATP-induced genes (Table 1). This pattern of gene expression suggests that eATP induces gene expression changes earlier and possibly faster than TGF-b, consistent with the observation that eATP induced faster morphological changes than TGF-b (Fig. 3 and [29]). This is also consistent with the notion of the multi-functionality and multi-locality of eATP.

Unlike the RNAseq profiles at 2 and 6 hours after the inductions, which reflected the changes in early and late stages of gene expression during EMT, the metabolomics profile represents changes at the metabolic and therefore phenotypic levels associated with EMT [44, 45]. The metabolomics data provides evidence, in addition to the RNAseq gene expression data, that eATP induced a gene expression and metabolic

profile similar to that induced by TGF-b (Fig. 2). The specific altered pathways and metabolite levels, compared with TGF-b, are clear indications that the metabolic state induced by eATP is similar to that induced by TGF-b, and is indeed a state corresponding to EMT.

These changes indicate that eATP induced pattern alterations from transcription to metabolic levels with characteristics expected for an induced EMT state, which is also similar to EMT state induced by TGF-b. These findings have never been reported before.

We recently reported the observation that eATP induced both migration and invasion [29]. Our current invasion assays further expand the study by showing dose-dependent comparison between eATP and TGF-b in not only A549 cells, but also in a second lung cancer cell line H1299 (Fig. 3a and 3b). The new result shows that this is not a single cell line phenomenon but a potentially prevalent activity of eATP among cancer cells. The doses of eATP used in this study were the same as the concentration range of eATP found in TME [16–19], implying its roles *in vivo*. Our subsequent fluorescent microscopy study revealed that the eATP treatment led to an earlier formation of filopodia-like protrusions in A549 and H1299 cells in a time-dependent manner (Fig. 4a and 4b) than TGF-b. This result provides a first piece of visual evidence for earlier EMT-related morphological changes induced by eATP.

Eleven genes, which were significantly upregulated and completely conserved in eATP and TGF-b treated cells at both 2 and 6 hours, were identified (Table 1). Several genes in this group, including Sox8, BMP6, MMP10, and IL-1A, are known to play roles in EMT. other genes including STC1, BLOC1S6, are not known to be involved in EMT. It is particularly interesting to find that ATP6V1G2, an untranslated long transcript fused between an ATPase gene and an RNA splicing gene, is also included in this group. The presence and conservation of ATP6V1G2 long RNA suggest the potential regulatory functions of the long transcript. The presence of the transcript in TGF-b treated cells also suggests that this is not an eATP-unique phenomenon. It is likely to be more fundamental for induction and regulation of EMT. It is also noteworthy that 8 out of the 11 (~ 73%) genes were induced to the higher level by eATP than TGF-b at 2 hours, while only 4 out 11 genes (~ 36%) were induced to the higher level by eATP than TGF-b at 6 hours. This provides another piece of evidence that eATP induces EMT earlier than TGF-b in addition to the invasion assay and then filopodia formation assay.

The study for the functional relationship revealed that eATP and TGF-b do not show an additive effect on invasion at higher (TME) concentrations (Fig. 5a and 5b), suggestive of the overlapping of the invasion-inducing activities of the two molecules. When pan-TGF-b neutralizing antibodies were exogenously added, diminished invasion was observed. The decrease was reversed, restored, and the viability was even enhanced by the addition of eATP (Fig. 5c and 5d). These results assert that ATP can not only induce invasion without the addition of TGF- b, but also in the absence of TGF- b induced signaling, further supporting the notion that eATP functions independent of TGF- b in the induction of EMT.

The faster EMT induction by eATP than TGF-b might be related to macropinocytosis-mediated ATP internalization, which results in a large elevation of intracellular ATP (iATP) levels. The ATP assay confirmed this speculation in that eATP induced large dose-dependent iATP elevations in both A549 and

H1299 cells, while TGF-b did not (Fig. 6a & 6b). It is conceivable that the highly elevated iATP enhanced protein phosphorylation in signal transduction, accelerated biochemical reactions and cell morphology changes, and increased cell motility. We previously demonstrated that some of these activities were blocked when macropinocytosis, a primary hallmark of cancer metabolism [49], was inhibited [29]. A549 and H1299 cells are known to exhibit macropinocytosis [50, 51]. In addition, iATP directly participates in induction and regulation of gene expressions in cancer cells as a transcriptional cofactor. All these combined together may account for the greater invasion rates compared with TGF-b (Fig. 3a & 3b). Many other cancer cell lines of other cancer types also show macropinocytosis [20–22]. Although macropinocytosis is an energy-consuming (ATP-consuming) process, our study implies that cancer cells use it to obtain sufficient “free” ATP from the TME to drive and sustain macropinocytosis and the biochemical reactions and protein phosphorylation without using as much endogenously synthesized ATP.

Based on all the previous studies related to ATP-induced EMT [14, 29] and this study, here we propose a significantly updated hypothetical model for how eATP induces and regulates EMT spatially and temporally in human lung cancers (Fig. 7e). First, eATP, at the concentration range found in TME [16–19], functions extracellularly by binding and activating various purinergic receptors (PR) located on plasma membrane, leading to PR-mediated specific signaling for EMT induction [39, 52]. Exactly which PR(s) are activated depend on the specific eATP concentration as different PRs have different affinities for ATP. This part of eATP activity is similar or identical to the mechanism of TGF-b mediated PR signaling as TGF-b induces ATP exocytosis and subsequent ATP-PR binding/activating (13–14) with the exception that eATP levels in the TME may be higher than the eATP level achieved by TGF-b -mediated ATP exocytosis. This is because eATP in the TME is from multiple sources [53, 54] in addition to TGF-b-induced exocytosis [13, 14]. Simultaneously with the PR signaling, eATP is also internalized by macropinocytosis [20–22, 25–27], greatly enhancing the level of intracellular ATP (iATP) by at least 30–50% within 2–3 hours [25–27]. The elevated iATP, in turn, accelerates all biochemical / enzymatic reactions inside the cell partly driven by ATP, including both ATP hydrolysis in metabolic reactions and protein phosphorylation in signal transduction. Furthermore, ATP is versatile transcriptional cofactor, directly participating in and augmenting gene expression by ways of double strand DNA unwinding, transcription initiation, elongation, and other steps in transcription [30–34]. All these processes working concurrently at different subcellular locations and at various levels of biological function result in induction and spatial and temporary regulation of EMT and steps beyond EMT in metastasis. While the specificity of the gene expression induced by eATP is likely to be originated from the PR signaling, the intensity of the gene expression is likely to be regulated by the other intracellular functions of eATP and potential negative feedback loops between gene transcription rates and enhanced enzymatic activities induced by augmented protein phosphorylation and/or faster enzymatic reactions (and therefore altered metabolite levels) driven by higher iATP levels. Thus, this model not only explains how eATP induces TGF-b-like EMT, but also explains why eATP induces EMT somewhat differently from TGF-b-induced EMT at the levels of transcription and biochemical reactions, resulting in earlier morphological / functional changes. Additional studies are needed for the final validation of this hypothetical model.

Conclusions

Taken together, eATP, which is abundantly present in the TME, is an evolutionarily conserved and selected but previously under-recognized molecule that has been emerging as a powerful inducer and regulator of EMT and potentially other steps of metastasis. Its roles in EMT are “amplified” by its internalization through macropinocytosis and subsequent drastic elevation of intracellular ATP levels. Results of this study not only demonstrate the multi-functional nature of eATP, but also reflect the flexibility of cancer cells, which are able to use either TGF-b or eATP or both, whichever is present in the TME at appropriate concentrations or in various ratios to induce EMT. The RNAseq and metabolomics analyses not only reveal the eATP induces EMT from expression of specific gene involved in EMT to representative metabolite changes similar to those induced by TGF-b. The functional assays further validate the results from transcriptomics and metabolomics. New findings documented in this study will compel us to rethink exactly how EMT is induced and regulated in tumors, and how it will enable us to develop novel and effective anticancer and anti-metastasis strategies by targeting eATP [55]. It also identifies eATP as a new economical and convenient tool, alternative to TGF-b, to dissect and investigate EMT and metastasis.

Abbreviations

EMT: Epithelial mesenchymal transition

eATP: Extracellular ATP

GSEA: Gene set enrichment analysis

ieATP: Intratumoral eATP

iATP: Intracellular ATP

TGF- b: Transforming growth factor beta

NES: Normalized enrichment score

NSCLC: Non-small cell lung carcinoma

PR: Purinergic receptor

TME: Tumor microenvironment

DMEM: Dulbecco’s Modified Eagle Medium

PLS-DA: Partial least squares-discriminant analysis

Log2fc: Log2 fold change

Declarations

Ethic approval: Not applicable

Consent to participate – not applicable

Consent for publication – not applicable

Availability of data and materials

RNA sequencing data have been deposited in https://www.ncbi.nlm.nih.gov/geo/subs/, with an accession number GSE160671. The data used for metabolomics analysis is available at the NIH Common Fund's National Metabolomics Data Repository (NMDR) website, the Metabolomics Workbench, https://www.metabolomicsworkbench.org where it has been assigned data track ID 2563. This work is supported by NIH grant U2C-DK119886.

Competing interests – Authors declare no competing interests.

Fund information – For ME, John J. Kopchick Award, Ohio University Student Enhancement Award, Ohio University Provost's Undergraduate Award, Ohio University Honors Tutorial College Dean's Research Fund. For PS, John J. Kopchick Award, Ohio University Student Enhancement Award. For XC, NIH grant R15 CA242177-01.

Authors' contributions

ME: Design and execution of most experiments related to functional assays, data analysis of RNAseq, figure generation, manuscript writing. JS: Performance of some RNAseq related experiments, writing and submission of manuscript. PS: Analysis of metabolomics data, generation of figures, and writing of manuscript. HSG: RNAseq data analysis. XC: Conceptualization and Design of the study, supervision and coordination of the study, participation in writing and submission of the manuscript, and major funding support of the study.

Acknowledgments

We thank Lindsey Bachmann for technical support, the Campus Chemical Instrumentation Center (CCIC) at the Ohio State University for performing LC-MS/MS metabolomics analysis and this work was supported by NIH Award Number Grant P30 CA016058. We also thank National Metabolomics Data Repository (NMDR) for providing the platform to upload the metabolomics dataset.

References

1. Lambert AW, Pattabiraman DR, Weinberg RA. Emerging Biological Principles of Metastasis. *Cell*. 2017;168(4):670-691. https://doi.org/10.1016/j.cell.2016.11.037

2. Nieto MA, Huang RY, Jackson RA, Thiery JP. EMT: 2016. *Cell*. 2016;166(1):21-45. https://doi.org/10.1016/j.cell.2016.06.028

3. Yang, J., Antin, P., Berx, G. et al. Guidelines and definitions for research on epithelial–mesenchymal transition. Nat Rev Mol Cell Biol 21, 341–352 (2020). https://doi.org/10.1038/s41580-020-0237-9

4. Lamouille S, Xu J, Derynck R. Molecular mechanisms of epithelial-mesenchymal transition. *Nat Rev Mol Cell Biol*. 2014;15(3):178-196. https://doi.org/10.1038/nrm3758

5. Lai X, Li Q, Wu F, Lin J, Chen J, Zheng H, and Guo L. Epithelial-Mesenchymal Transition and Metabolic Switching in Cancer: Lessons From Somatic Cell Reprogramming. Front. Cell Dev. Biol., 06 August 2020 | https://doi.org/10.3389/fcell.2020.00760

6. Dongre A, Weinberg RA. New insights into the mechanisms of epithelial-mesenchymal transition and implications for cancer. *Nat Rev Mol Cell Biol*. 2019;20(2):69-84. https://doi.org/10.1038/s41580-018-0080-4

7. Saitoh M. Involvement of partial EMT in cancer progression. *J Biochem*. 2018;164(4):257-264. https://doi.org/10.1093/jb/mvy047

8. Aiello NM, Maddipati R, Norgard RJ, et al. EMT Subtype Influences Epithelial Plasticity and Mode of Cell Migration. *Dev Cell*. 2018;45(6):681-695.e4. https://doi.org/10.1016/j.devcel.2018.05.027

9. Hao Y, Baker D, Ten Dijke P. TGF-β-Mediated Epithelial-Mesenchymal Transition and Cancer Metastasis. *Int J Mol Sci*. 2019;20(11):2767. Published 2019 Jun 5. https://doi.org/10.3390/ijms20112767

10. Xu J, Lamouille S, Derynck R. TGF-beta-induced epithelial to mesenchymal transition. *Cell Res*. 2009;19(2):156-172. https://doi.org/10.1038/cr.2009.5

11. Hua, W., ten Dijke, P., Kostidis, S. et al. TGFβ-induced metabolic reprogramming during epithelial-to-mesenchymal transition in cancer. Cell. Mol. Life Sci. 77, 2103–2123 (2020). https://doi.org/10.1007/s00018-019-03398-6

12. Ferrarelli, L. Revisiting TGF-β and EMT. *2019; 363*;941-943. https://doi.org/10.1126/science.363.6430.941-s

13. Martínez-Ramírez AS, Díaz-Muñoz M, Butanda-Ochoa A, Vázquez-Cuevas FG. Nucleotides and nucleoside signaling in the regulation of the epithelium to mesenchymal transition (EMT). *Purinergic Signal*. 2017;13(1):1-12. https://doi.org/10.1007/s11302-016-9550-3

14. Yang H, Geng YH, Wang P, et al. Extracellular ATP promotes breast cancer invasion and epithelial-mesenchymal transition via hypoxia-inducible factor 2α signaling. *Cancer Sci*. 2019;110(8):2456-2470. https://doi.org/10.1111/cas.14086

15. Takai E, Tsukimoto M, Harada H, Kojima S. Autocrine signaling via release of ATP and activation of P2X7 receptor influences motile activity of human lung cancer cells. *Purinergic Signal*. 2014;10(3):487-497. https://doi.org/10.1007/s11302-014-9411-x

16. Pellegatti P, Raffaghello L, Bianchi G, Piccardi F, Pistoia V, Di Virgilio F. Increased level of extracellular ATP at tumor sites: in vivo imaging with plasma membrane luciferase. *PLoS One*. 2008;3(7):e2599. https://doi.org/10.1371/journal.pone.0002599

17. Wilhelm K, Ganesan J, Müller T, et al. Graft-versus-host disease is enhanced by extracellular ATP activating P2X7R. *Nat Med*. 2010;16(12):1434-1438. https://doi.org/10.1038/nm.2242

18. Michaud M, Martins I, Sukkurwala AQ, et al. Autophagy-dependent anticancer immune responses induced by chemotherapeutic agents in mice. *Science*. 2011;334(6062):1573-1577. https://doi.org/10.1126/science.1208347

19. Di Virgilio, F., Adinolfi, E. Extracellular purines, purinergic receptors and tumor growth. Oncogene 36, 293–303 (2017). https://doi.org/10.1038/onc.2016.206

20. Commisso C, Davidson SM, Soydaner-Azeloglu RG, et al. Macropinocytosis of protein is an amino acid supply route in Ras-transformed cells. *Nature*. 2013;497(7451):633-637. https://doi.org/10.1038/nature12138

21. Commisso C. The pervasiveness of macropinocytosis in oncological malignancies. *Philos Trans R Soc Lond B Biol Sci*. 2019;374(1765):20180153. https://doi.org/10.1098/rstb.2018.0153

22. Swanson JA, King JS. The breadth of macropinocytosis research. *Philos Trans R Soc Lond B Biol Sci*. 2019;374(1765):20180146. https://doi.org/10.1098/rstb.2018.0146

23. Liu Y, Zhang W, Cao Y, Liu Y, Bergmeier S, Chen X. Small compound inhibitors of basal glucose transport inhibit cell proliferation and induce apoptosis in cancer cells via glucose-deprivation-like mechanisms. *Cancer Lett*. 2010;298(2):176-185. https://doi.org/10.1016/j.canlet.2010.07.002

24. Liu Y, Cao Y, Zhang W, et al. A small-molecule inhibitor of glucose transporter 1 downregulates glycolysis, induces cell-cycle arrest, and inhibits cancer cell growth in vitro and in vivo. *Mol Cancer Ther*. 2012;11(8):1672-1682. https://doi.org/10.1158/1535-7163.MCT-12-0131

25. Qian Y, Wang X, Liu Y, et al. Extracellular ATP is internalized by macropinocytosis and induces intracellular ATP increase and drug resistance in cancer cells. *Cancer Lett*. 2014;351(2):242-251. https://doi.org/10.1016/j.canlet.2014.06.008

26. Qian Y, Wang X, Li Y, Cao Y, Chen X. Extracellular ATP a New Player in Cancer Metabolism: NSCLC Cells Internalize ATP In Vitro and In Vivo Using Multiple Endocytic Mechanisms. *Mol Cancer Res*. 2016;14(11):1087-1096. https://doi.org/10.1158/1541-7786.MCR-16-0118

27. Wang X, Li Y, Qian Y, et al. Extracellular ATP, as an energy and phosphorylating molecule, induces different types of drug resistances in cancer cells through ATP internalization and intracellular ATP level increase. *Oncotarget*. 2017;8(50):87860-87877. https://doi.org/10.18632/oncotarget.21231

28. Wang X, Zhang H, Chen X. Drug resistance and combating drug resistance in cancer. Cancer Drug Resistance.2019. https://doi.org/20517/cdr.2019.10

29. Cao Y, Wang X, Li Y, Evers M, Zhang H, Chen X. Extracellular and macropinocytosis internalized ATP work together to induce epithelial-mesenchymal transition and other early metastatic activities in lung cancer. *Cancer Cell Int*. 2019;19:254. https://doi.org/10.1186/s12935-019-0973-0

30. Dvir A, Garrett KP, Chalut C, Egly JM, Conaway JW, Conaway RC. A role for ATP and TFIIH in activation of the RNA polymerase II preinitiation complex prior to transcription initiation. *J Biol Chem*. 1996;271(13):7245-7248. https://doi.org/10.1074/jbc.271.13.7245

31. Conaway RC, Conaway JW. ATP activates transcription initiation from promoters by RNA polymerase II in a reversible step prior to RNA synthesis. *J Biol Chem*. 1988;263(6):2962-2968.

32. Porrua O, Libri D. Transcription termination and the control of the transcriptome: why, where and how to stop. *Nat Rev Mol Cell Biol*. 2015;16(3):190-202. https://doi.org/10.1038/nrm3943

33. Fishburn J, Galburt E, Hahn S. Transcription Start Site Scanning and the Requirement for ATP during Transcription Initiation by RNA Polymerase II. *J Biol Chem*. 2016;291(25):13040-13047. https://doi.org/10.1074/jbc.M116.724583

34. Wang W, Carey M, Gralla JD. Polymerase II promoter activation: closed complex formation and ATP-driven start site opening. *Science*. 1992;255(5043):450-453. https://doi.org/10.1126/science.1310361

35. Ashburner M, Ball CA, Blake JA, et al. Gene ontology: tool for the unification of biology. The Gene Ontology Consortium. Nat Genet. 2000;25(1):25-29. doi:10.1038/75556

36. The Gene Ontology Consortium, The Gene Ontology resource: enriching a GOld mine, Nucleic Acids Research, 2021, 49(D1):D325-D334.

37. Subramanian A, Tamayo P, Mootha VK, Mukherjee S, Ebert BL, Gillette MA, Paulovich A, Pomeroy SL, Golub TR, Lander ES, Mesirov JP. Gene set enrichment analysis: a knowledge-based approach for interpreting genome-wide expression profiles. Proc Natl Acad Sci U S A. 2005 Oct 25;102(43):15545-50. doi: 10.1073/pnas.0506580102.

38. Mootha, V., Lindgren, C., Eriksson, KF. et al. PGC-1α-responsive genes involved in oxidative phosphorylation are coordinately downregulated in human diabetes. Nat Genet 34, 267–273 (2003). https://doi.org/10.1038/ng1180

39. Liberzon A, Subramanian A, Pinchback R, Thorvaldsdóttir H, Tamayo P, Mesirov JP. Molecular signatures database (MSigDB) 3.0. Bioinformatics. 2011 Jun 15;27(12):1739-40. doi: 10.1093/bioinformatics/btr260.

40. Huang DW, Sherman BT, Lempicki RA. Systematic and integrative analysis of large gene lists using DAVID Bioinformatics Resources. Nature Protoc. 2009;4(1):44-57. doi: 10.1038/nprot.2008.211

41. Huang DW, Sherman BT, Lempicki RA. Bioinformatics enrichment tools: paths toward the comprehensive functional analysis of large gene lists. Nucleic Acids Res. 2009;37(1):1-13. doi: 10.1093/nar/gkn923

42. Shriwas P, Roberts D, Li Y, Wang L, Qian Y, Bergmeier S, Hines J, Adhicary S, Neilsen C, Chen X. A small-molecule pan-class I glucose transporter inhibitor reduces cancer cell proliferation in vitro and tumor growth in vivo by targeting glucose-based metabolism. Cancer Metab, 2021;9(14). https://doi.org/10.1186/s40170-021-00248-7

43. Yamada H, Takeda T, Michiue H, Abe T, Takei K. Actin bundling by dynamin 2 and cortactin is implicated in cell migration by stabilizing filopodia in human non-small cell lung carcinoma cells. *Int J Oncol*. 2016;49(3):877-886. https://doi.org/10.3892/ijo.2016.3592

44. Kang H, Kim H, Lee S, Youn H, Youn B. Role of Metabolic Reprogramming in Epithelial‐Mesenchymal Transition (EMT). *Int J Mol Sci*. 2019;20(8):2042. https://doi.org/10.3390/ijms20082042

45. Georgakopoulos-Soares I, Chartoumpekis DV, Kyriazopoulou V, Zaravinos A. EMT Factors and Metabolic Pathways in Cancer. *Front Oncol*. 2020;10:499. https://doi.org/10.3389/fonc.2020.00499

46. Di Virgilio F, Sarti AC, Falzoni S, De Marchi E, Adinolfi E. Extracellular ATP and P2 purinergic signalling in the tumour microenvironment. *Nat Rev Cancer*. 2018;18(10):601-618. https://doi.org/10.1038/s41568-018-0037-0

47. Di Virgilio F, Pinton P, Falzoni S. Assessing Extracellular ATP as Danger Signal In Vivo: The pmeLuc System. *Methods Mol Biol*. 2016;1417:115-129. https://doi.org/10.1007/978-1-4939-3566-6_7

48. Ding Q, Tan KS. The Danger Signal Extracellular ATP Is an Inducer of *Fusobacterium nucleatum* Biofilm Dispersal. *Front Cell Infect Microbiol*. 2016;6:155. https://doi.org/10.3389/fcimb.2016.00155

49. Pavlova NN, Thompson CB. The Emerging Hallmarks of Cancer Metabolism. *Cell Metab*. 2016;23(1):27-47. https://doi.org/10.1016/j.cmet.2015.12.006

50. Yumoto R, Suzuka S, Oda K, Nagai J, Takano M. Endocytic uptake of FITC-albumin by human alveolar epithelial cell line A549. *Drug Metab Pharmacokinet*. 2012;27(3):336-343. https://doi.org/10.2133/dmpk.dmpk-11-rg-127

51. Hodakoski C, Hopkins BD, Zhang G, et al. Rac-Mediated Macropinocytosis of Extracellular Protein Promotes Glucose Independence in Non-Small Cell Lung Cancer. *Cancers (Basel)*. 2019;11(1):37. https://doi.org/10.3390/cancers11010037

52. Burnstock G, Di Virgilio F. Purinergic signalling and cancer. *Purinergic Signal*. 2013;9(4):491-540. https://doi.org/10.1007/s11302-013-9372-5

53. Di Virgilio F, Dal Ben D, Sarti AC, Giuliani AL, Falzoni S. The P2X7 Receptor in Infection and Inflammation. *Immunity*. 2017;47(1):15-31. https://doi.org/10.1016/j.immuni.2017.06.020

54. Kroemer G, Galluzzi L, Kepp O, Zitvogel L. Immunogenic cell death in cancer therapy. *Annu Rev Immunol*. 2013;31:51-72. https://doi.org/10.1146/annurev-immunol-032712-100008

55. Vultaggio-Poma V, Sarti AC, Di Virgilio F. Extracellular ATP: A Feasible Target for Cancer Therapy. Cells 2020, 9, 2496; doi:10.3390/cells9112496

Table

Due to technical limitations, the table is only available as a download in the supplemental files section.

Figures

FIG. 1

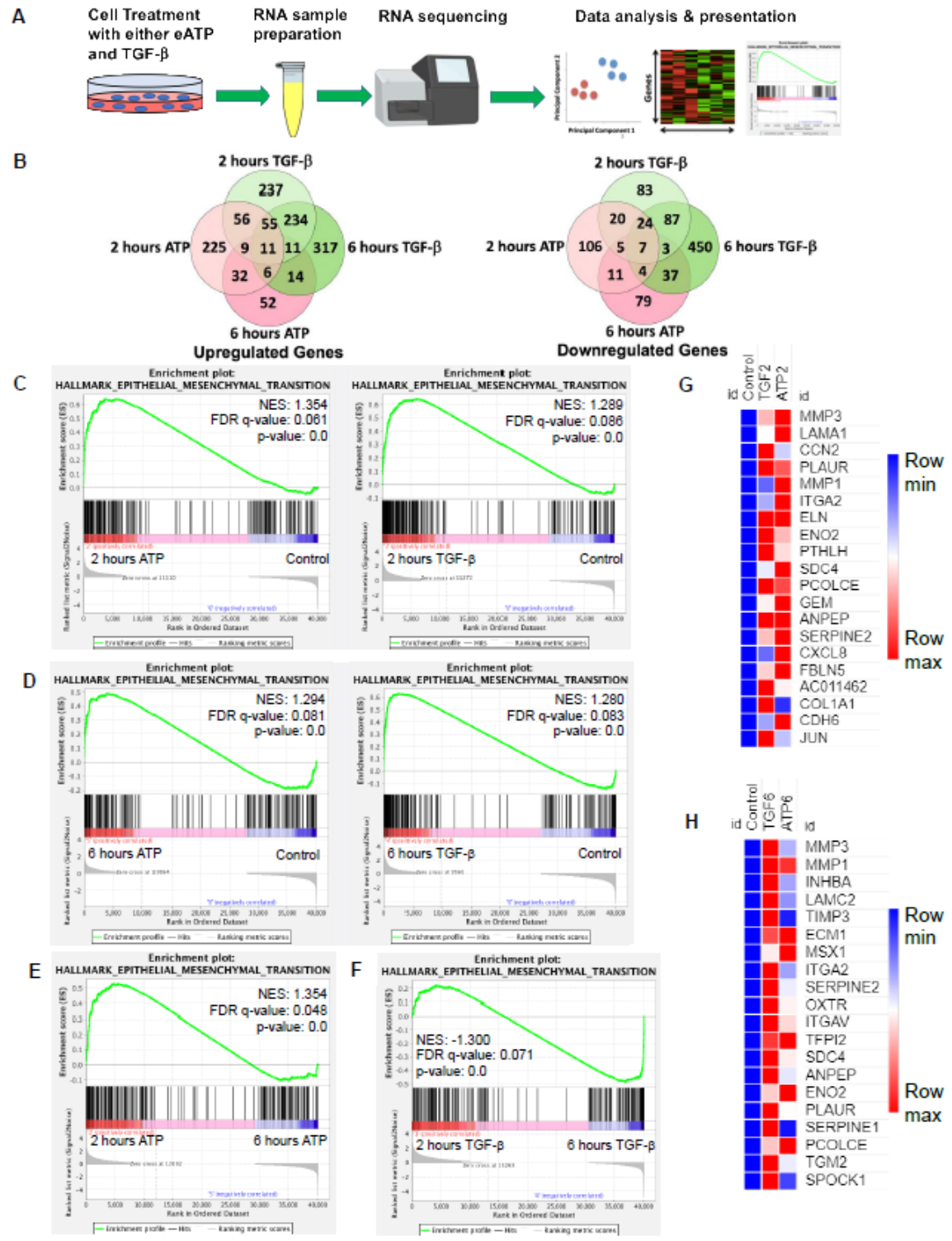

Figure 1

A549 cells were treated with either 0.5 mM ATP or 10 ng/mL TGF-β for 2 or 6 hours. After the treatment, polyA-containing RNA was isolated and then sent to a commercial service company for RNAseq analysis as described in detail in the Materials and Methods. The general RNAseq results are presented in Venn diagrams, GSEA plots, and heatmaps. NES: normalized enrichment score. a. Workflow for RNA-sequencing study. b. Venn Diagram of genes significantly upregulated (left) or downregulated (right) by

either ATP or TGF-β at 2 or 6 hours. c. Gene set enrichment analysis (GSEA) plots for the “Hallmark - Epithelial mesenchymal transition” signature, 2 hours ATP compared to control (left) and 2 hours TGF-β compared to control (right). d-f: GSEA plots for the “Hallmark - Epithelial mesenchymal transition” signature. (d) 6 hours ATP compared to control (left) and 6 hours TGF-β compared to control (right). (e) 2 hours ATP compared to 6 hours ATP. (f) 2 hours TGF-β compared to 6 hours TGF-β. g-h: Heatmap showing top 20 enriched genes from the “Hallmark - Epithelial mesenchymal transition” signature in (g) 2 hours ATP and 2 hours TGF-β and (h) 6 hours ATP and 6 hours TGF-β.

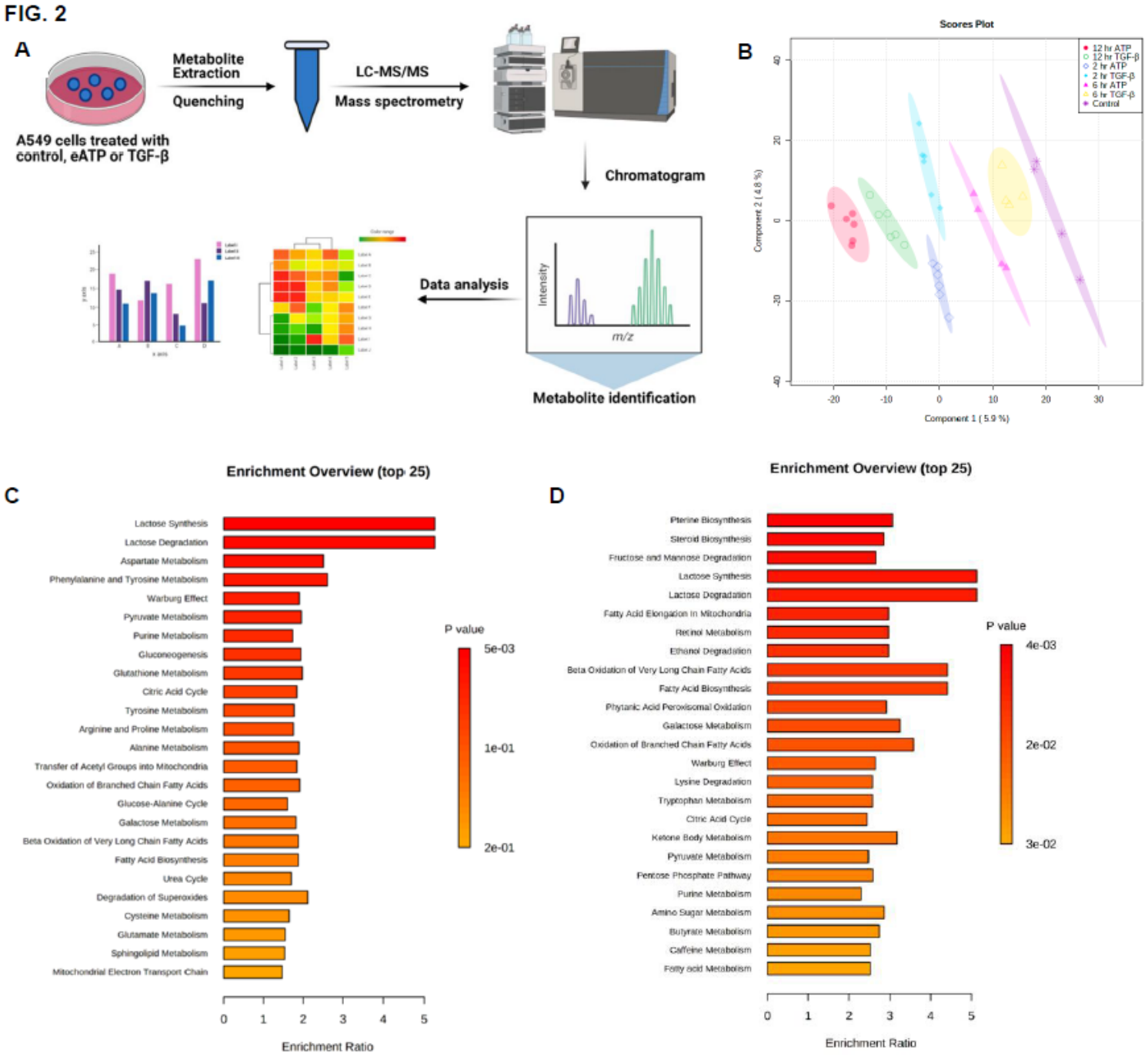

Figure 2

Metabolomics analysis of metabolic changes induced by eATP A549 cells were treated with either ATP or TGF-β for 0 (control), 2, 6 and 12 hours. Specially prepared cell lysates were subjected to a metabolomics analysis as described in Materials and Methods. The metabolomics data were presented in different ways to show their EMT-related features, similarities between ATP and TGF-β, and differences from the control. a. Schematic presentation of the design of the metabolomics study. b. PLS-DA plot for eATP or TGF-β treated samples at different treatment times as compared to the untreated control. c and d. Metabolic pathway enrichment analysis of ATP treatment at 2 hr (c), and enrichment by TGF-β at 2 hr (d).

FIG. 3

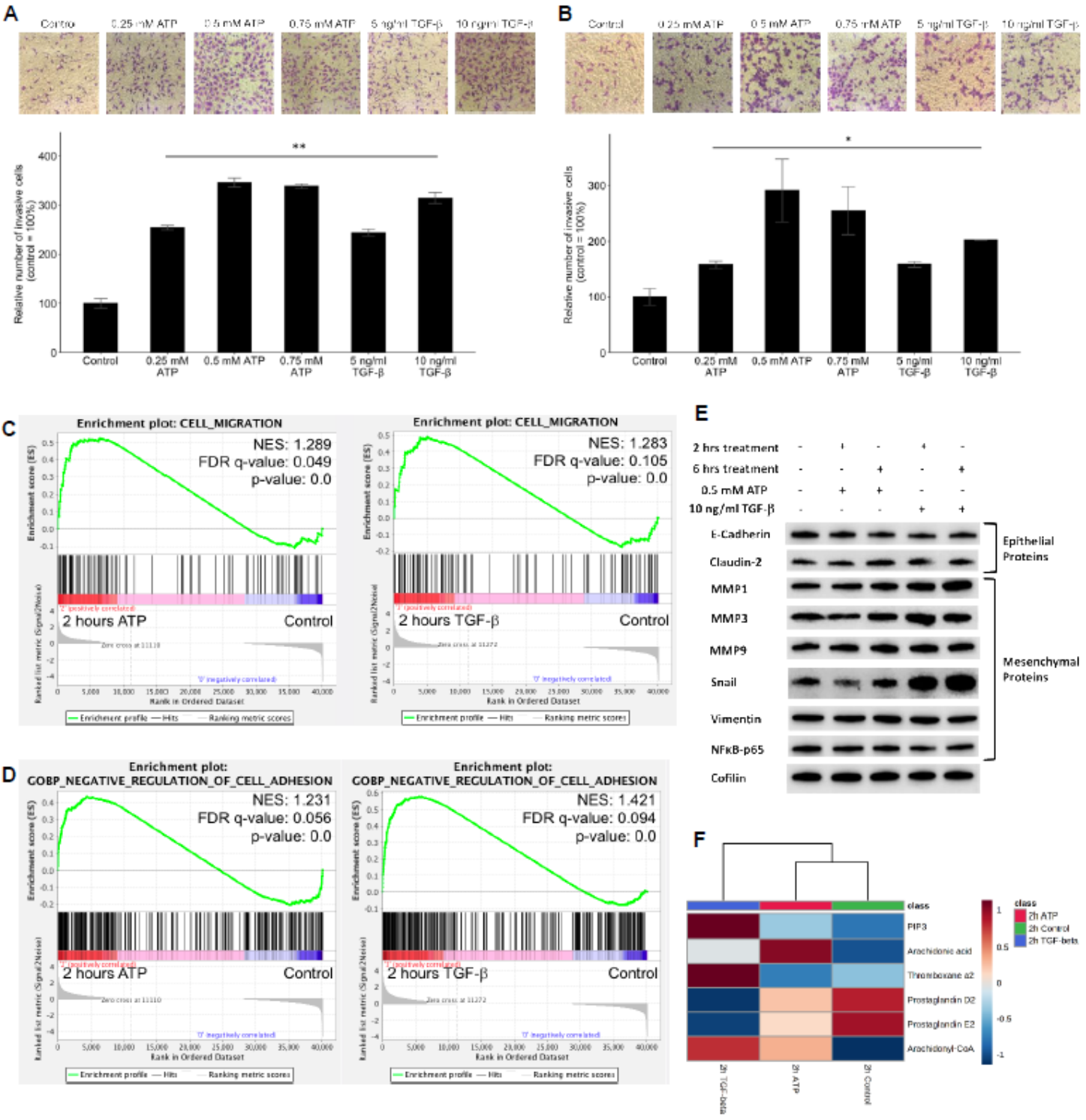

Figure 3

Extracellular ATP induces dose-dependent invasion faster than TGF-β Human NSCLC A549 and H1299 cells were grown in Transwells with collagen Matrigel coated membranes for 20 hours (invasion assay) in the presence or absence of ATP or TGF-β at various concentrations. After the treatment, invaded cells were fixed, stained, and visually counted and averaged. RNAseq analysis was used to identify corresponding gene expression changes. GSEA plots for the “cell migration” and “negative regulation of cell adhesion” signatures were performed to match/verify the observed phenotypic changes. NES: normalized enrichment score. * P < 0.05, ** P < 0.01. *** P < .001. a and b. eATP and TGF-β induce cell invasion in A549 cells (a) and in H1299 cells (b) c. GSEA plots, 2 hours ATP compared to control (left) and 2 hours TGF-β compared to control (right). d. GSEA plots for the “Negative regulation of cell adhesion” signature, 2 hours ATP compared to control (top) and 2 hours TGF-β compared to control (bottom). e. Western blot analysis of selected proteins related to EMT. Cofilin served as a loading control. f. Metabolomics heatmap for 6 metabolites involved in cell migration in differently treated cells.

FIG. 4

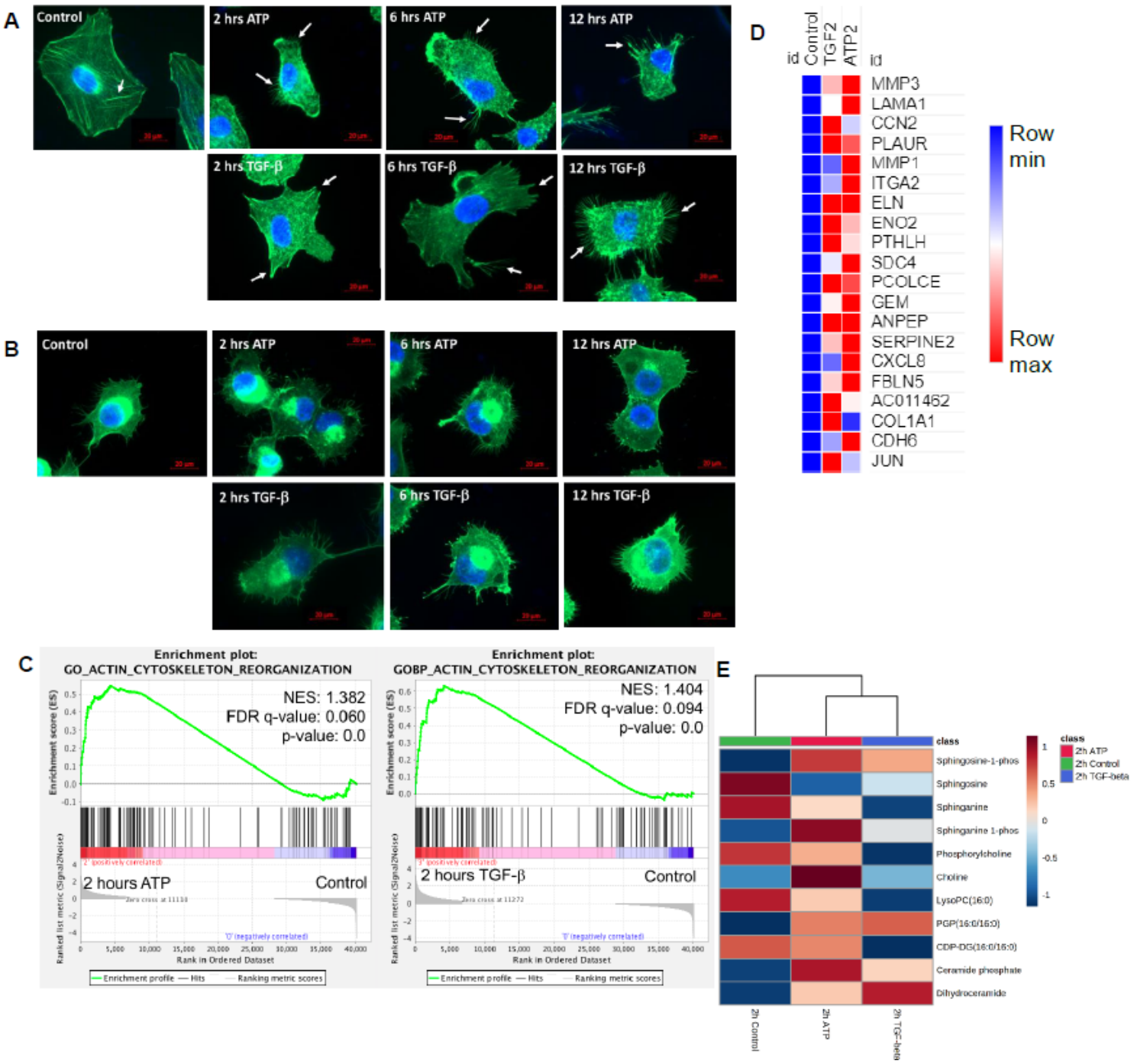

Figure 4

Extracellular ATP induces time-dependent formation of filopodia earlier than TGF-β confirmed by transcriptomics and metabolomics analyses. Human NSCLC A549 and H1299 cells were grown on coverslips in cell culture plates were treated with either eATP or TGF-β for various hours. After treatment, fluorescence microscopy was used to visualize time-dependent formation of filopodia-like protrusions in eATP- or TGF-β-treated A549 and H1299 cells. NES: normalized enrichment score. a and b. Fluorescence microscopy of time-dependent formation of filopodia-like protrusion formation in eATP-treated A549 cells (a) and H1299 cells (b). Untreated and TGF-β treated cells served as negative and positive controls.

Arrows point to distinctive protrusions of the cells. c. Transcriptomics GSEA plots for the “GO Actin Cytoskeleton Reorganization” signature derived from RNAseq data, 2 hours ATP compared to control (top) and 2 hours TGF-βcompared to control (bottom). d. Heat mal of the top 20 enriched genes in common between ATP and TGF-β for actin cytoskeleton reorganization. e. Heatmap of metabolomics analysis showing metabolites involved in actin cytoskeletal rearrangement altered by ATP and TGF-β in A549 cancer cells after 2 hours of treatment.

FIG. 5

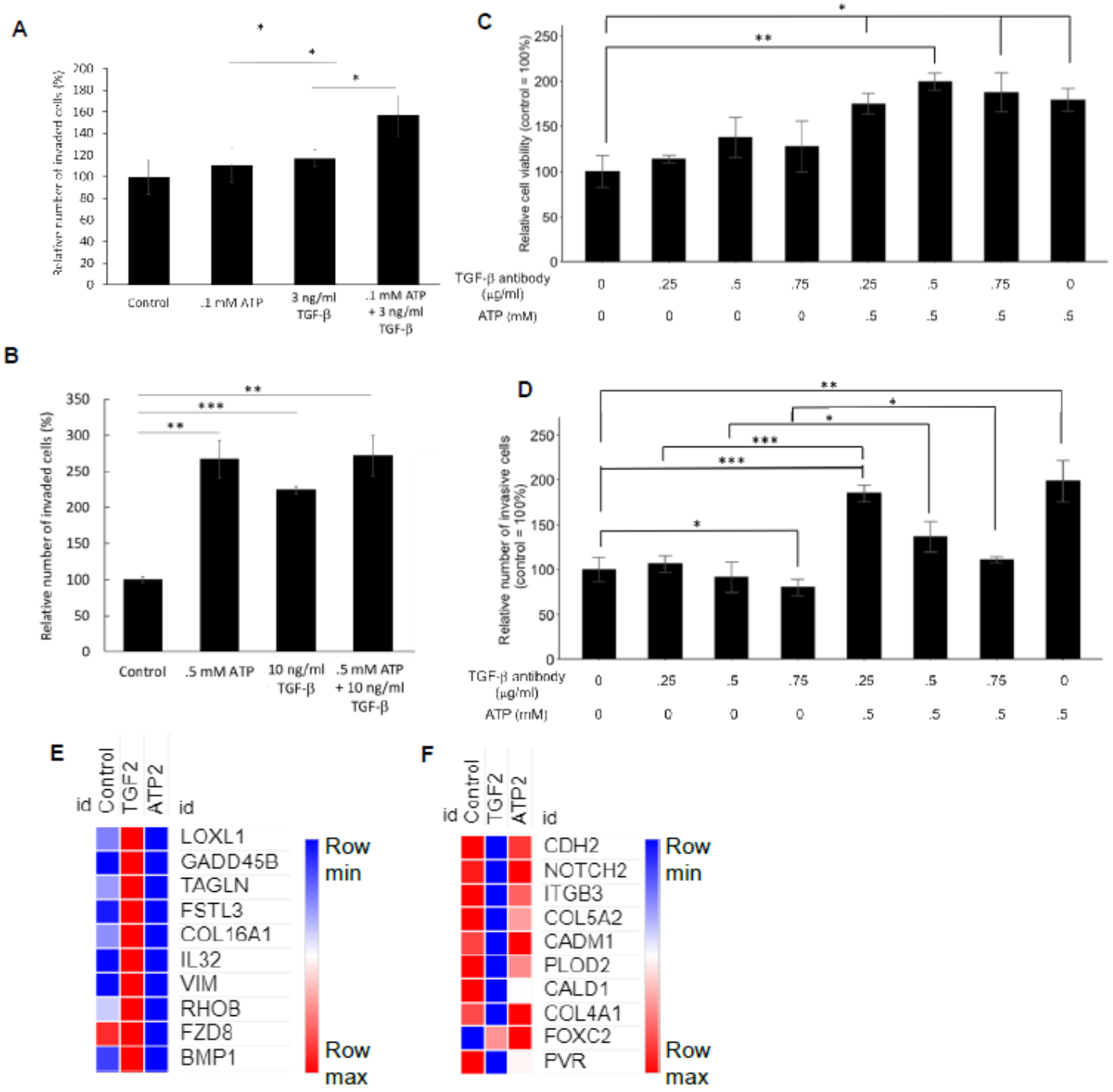

Figure 5

Mechanism study I: Similarities and differences in EMT induced by eATP or TGF-β. Human NSCLC A549 and/or H1299 cells grown in either regular cell culture plates or transwell plates were treated with either ATP, TGF-β, or both at various concentrations and measured for their respective intracellular ATP levels or additive effect in the invasion assay. In a different study, A549 cells were treated with anti-TGF-β neutralizing antibody at various concentrations in the presence or absence of different concentrations of eATP. 24 hours after the treatment, treated cells were assayed for their intracellular ATP levels or their cell viability by resazurin assay. * $P < 0.05$, ** $P < 0.01$. *** $P < .001$. a and b. eATP and TGF-β show an additive effect in inducing invasion at lower concentrations (a) while eATP and TGF-β do not show an additive effect in inducing invasion at higher concentrations (b). c and d. Extracellular ATP increased cell viability of cells treated with TGF-β neutralizing antibody (c). Extracellular ATP restored the invasiveness of A549 cells treated with TGF-β antibody (d) in A549 cells. e and f. Heatmaps of EMT-related genes upregulated by TGF-b at 2 hours (e), and EMT-related genes upregulated by ATP at 2 hours (f).

FIG. 6

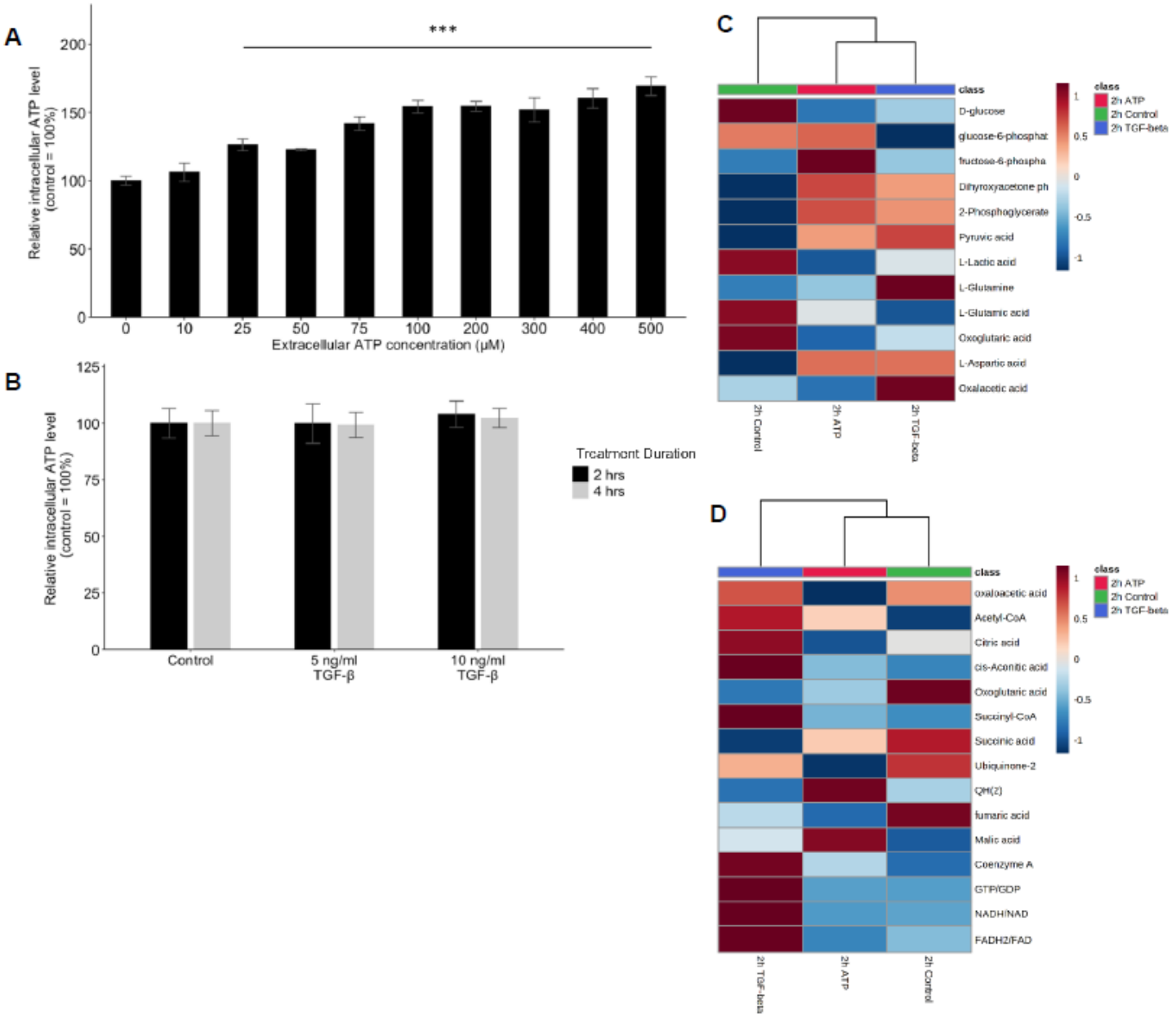

Figure 6

Mechanism study II: similarity and difference between eATP and TGF-β in intracellular ATP and in ATP synthesis-related metabolites. A549 cells were treated with either various concentrations of ATP or TGF-β. 24 hours after the treatment, cells were lysed and measured for their intracellular ATP concentrations. A549 cells were also treated by ATP and TGF-b for 2 hours and then their specific metabolites analyzed. * P < 0.05, ** P < 0.01. *** P < .001. a and b. Intracellular ATP levels of cells treated by various concentrations of ATP (a) and TGF-β(b). c and d. Heatmaps of concentrations of metabolites involved in glycolysis (c) or TCA cycle (d) in cells treated with ATP or TGF-β for 2 hours compared with the untreated control.

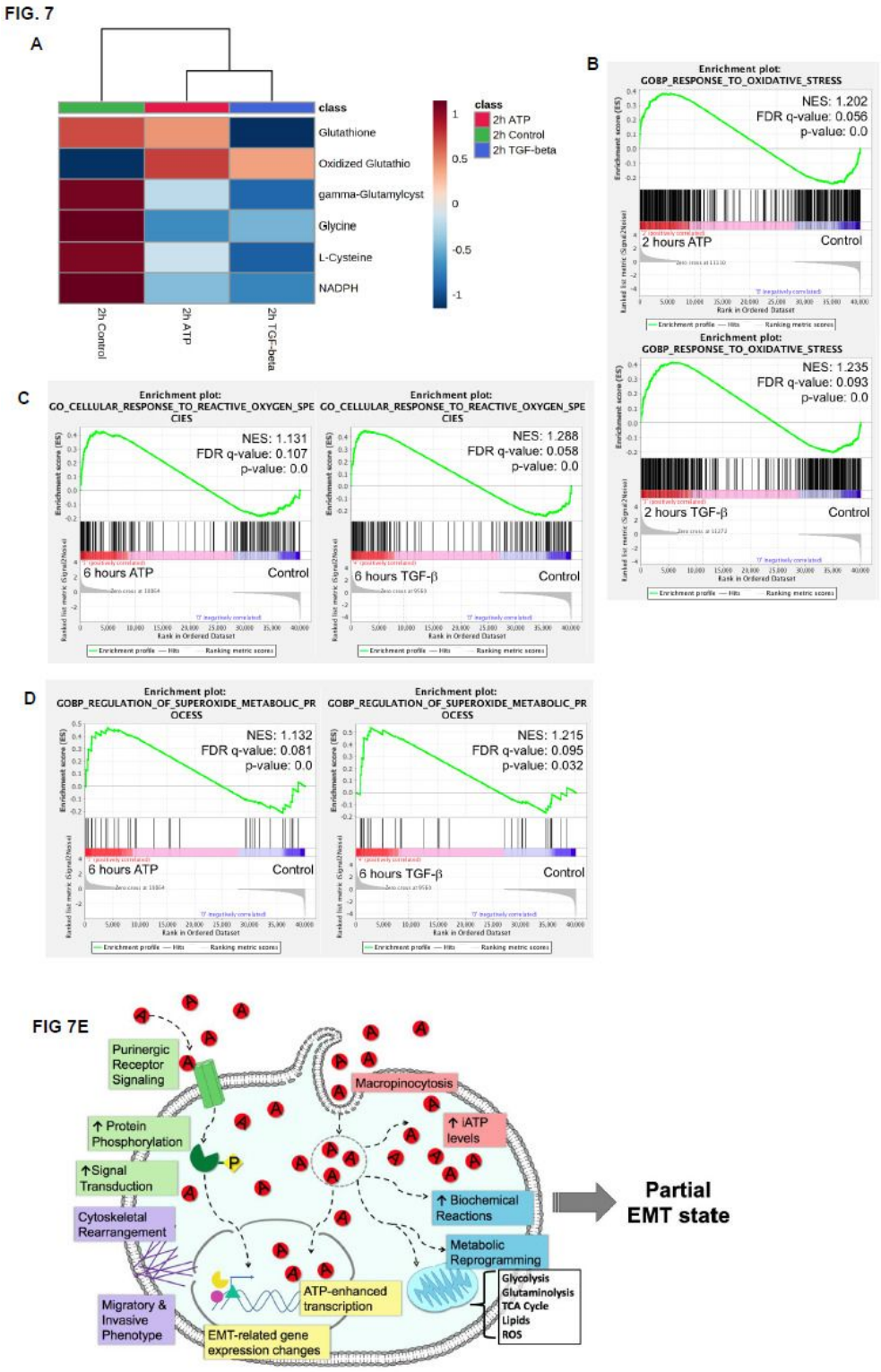

Figure 7

Mechanism study III: similarity and difference between eATP and TGF-β in ROS-related metabolites and genes. A549 cells were treated with either ATP or TGF-β for 2 hours. Then analyzed for their respective transcriptome and metabolome profiles. a. Heatmap of metabolomics analysis of concentrations of major metabolites in the ROS pathway. b-d. GSEA of RNAseq data for the enrichment of oxidative stress (b), cellular response to ROS (c), and superoxide metabolism (d). e. A hypothetical model for the

mechanisms used by eATP to induce EMT. Detailed explanation for the model can be found in Discussion.

Supplementary Files

This is a list of supplementary files associated with this preprint. Click to download.

- FinalSupplementaryfigs04062021.docx
- cm2021.4.6tablefile.docx